

## IRON OXIDE RECOVERY FROM FAYALITE IN WATER VAPOR AT HIGH TEMPERATURE

J.H. Chen <sup>a</sup>, W.J. Mi <sup>a</sup>, H.Y. Chen <sup>a</sup>, B. Li <sup>a</sup>, K.C. Chou <sup>b</sup>, X.M. Hou <sup>b,\*</sup>

<sup>a</sup> School of Material Science and Engineering, University of Science and Technology Beijing, China

<sup>b\*</sup> State Key Laboratory of Advanced Metallurgy, University of Science and Technology, Beijing, China

(Received 29 September 2016; accepted 23 May 2017)

### Abstract

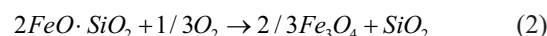
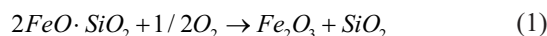
The oxidation behavior of fayalite ( $Fe_2SiO_4$ ) in water vapor at 1000°C was investigated. The phase constitution and microstructure of the solid products were characterized using X-ray diffraction (XRD) and scanning electron microscopy (SEM) with energy dispersive spectrometer (EDS). The gas product was continuously measured online by a gas analyzer. The results showed that fayalite was completely decomposed into magnetite (58.8 wt%), hematite (21.6 wt%) and silica (19.6 wt%) at 1000 °C for 40 min under water vapor condition. Compared with the result obtained in dry air, water vapor could promote fayalite to transform into magnetite by decreasing oxygen fugacity. In addition, the iron oxide product was further enriched via alkaline cleaning in 1 mol/L NaOH. As for the gas product, the hydrogen production capacity reached 24.41 mL/g when exposed to 50 vol% water-50 vol% Ar at 1000°C for 40 min.

**Keywords:** Fayalite; Water vapor; Oxidation behavior; Hydrogen; Magnetite

### 1. Introduction

Copper slag usually contains a certain quantity of valuable metals, such as copper, cobalt and iron [1-5]. Large amounts of copper slag generally contain about 40 wt% iron [5-6], which is higher than the average iron grade of iron ores (32% Fe) in China [7]. In this context, it is a valuable secondary iron resource for recycling and utilization. Therefore recovery of iron from the waste copper slag is of great interest for comprehensive use of mineral resource and reduction of environmental problems. It is known that most of iron in copper slag exists in form of fayalite ( $Fe_2SiO_4$ ) [8-10]. Fayalite is the iron-rich end member of the solid solution series  $Fe_2SiO_4$ - $Mg_2SiO_4$ , which belongs to the olivine mineral group (orthorhombic structure) [11-12]. In fayalite, Fe cations have the ferrous form ( $Fe^{2+}$ ) [13], which could either be transformed into magnetite and/or hematite mixture under oxidation condition or be reduced to metal Fe (FeO) under reducing atmosphere. Research shows that fayalite is difficult to be reduced to metallic iron by C and CO [14]. Additionally, there are reports explaining that it is preferable to convert fayalite to magnetite rather than metallic iron because the reduction of iron oxides to metallic iron is an endothermic reaction [15]. Therefore, the oxidation process is widely used in iron recovery, many studies proved that the ideal method

of recovering iron from copper slag involves the following two steps [8, 16-20]. Firstly, transfer  $Fe^{2+}$  from fayalite into  $Fe^{3+}$  from magnetite at high temperature. Secondly to separate them from slag by magnetic separation. The above process actually involves the oxidation and decomposition of fayalite. Systematic experimental and theoretical work have been carried out on the oxidation behavior of fayalite above 700 °C under various oxidizing conditions including air and different mixed atmosphere [21-23]. It is well known that the solid products of fayalite after oxidation are hematite ( $Fe_2O_3$ ), magnetite ( $Fe_3O_4$ ) and silica ( $SiO_2$ ) according to the following equations [24]:



Under above oxidizing conditions, iron oxide mainly exists in the form of hematite with little amount of magnetite as the intermediate product due to the high oxygen partial pressure. In contrast to the oxidation of fayalite under above oxidizing conditions, the reaction behavior of fayalite exposed to water vapor at high temperature is less discussed. Water vapor can promote fayalite to transform into magnetite by maintaining a low oxygen partial pressure. In addition, it is reported that water vapor

\*Corresponding author: houxinmeiustb@ustb.edu.cn



can promote the oxidation process of non-oxide material due to its specific inward diffusion mechanism [25]. Therefore it is supposed that water can also enhance the oxidation process of fayalite. At the same time, the gas product,  $H_2$  is supposed be used as a renewable energy. In this work, fayalite was exposed to water vapor at high temperature. The phase and microstructure evolution of the solid products were systematically investigated. At the same time, hydrogen concentration was in-situ measured. As for iron separation, an alkaline leaching process is selected to enrich the iron oxide and separate the iron oxide from  $SiO_2$ . This can solve the problem that magnetic separation cannot recover all iron oxide. It is a basic investigation of the oxidation behavior and reaction mechanism of fayalite in water vapor with the aim of the recovery of iron oxide from fayalite which could be used as the iron concentrate, catalyst, and abrasive materials.

## 2. Methods

### 2.1. Fayalite preparation

Fayalite used in this work was synthesized via solid reaction sintering method using analytically pure  $Fe_3O_4$  ( $\omega(Fe_3O_4) > 99.5\%$ ) and analytically pure  $SiO_2$  ( $\omega(SiO_2) > 99.3\%$ ) as raw materials.  $Fe_3O_4$  and  $SiO_2$  in the stoichiometric ratio were mixed by ball milling for 2 h using ethanol as the medium. The slurry was dried subsequently and pressed into specimens with size of  $\Phi 20 \text{ mm} \times 20 \text{ mm}$  under 10 MPa. The obtained specimens were embedded in analytically pure metal Fe powders to prevent pre-oxidation during heating process. Then they were placed into a furnace and heated slowly to 1150 °C for 5 h in air. The purpose of embedding the specimen with pure metal Fe powders is to form reducing atmosphere, which contributes to the formation of FeO. From the thermodynamical viewpoints, the coexistence phase with FeO is  $Fe_3O_4$

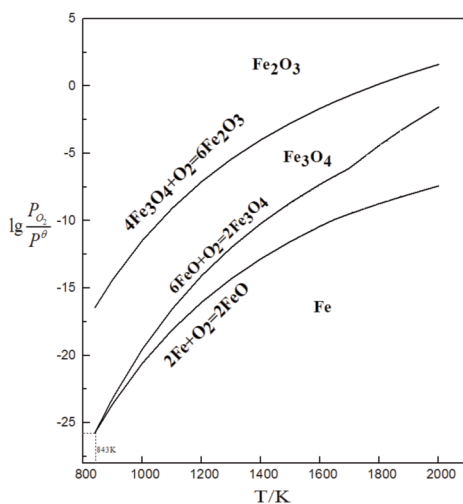


Figure 1. Thermodynamically stable area of Fe-O system

or Fe when the temperature is higher than 570 °C according to the stable area of Fe-O system as shown in Fig. 1. When the specimen is embedded in pure metal Fe powders, the iron source is sufficient. Only Fe can coexist with FeO. With temperature increasing, the metal iron powders tend to react with oxygen in the air to form a complete oxide layer, making the specimen completely be isolated from the outside. This makes the oxygen in the sample cannot exchange with the outside and forms a self-supporting system. Finally oxygen and (FeO) in the system is in a state of equilibrium, i.e.  $Fe + [O] \rightarrow (FeO)$ . Therefore (FeO) reacts quickly with  $SiO_2$  to generate  $Fe_2SiO_4$ .

### 2.2. Oxidation experiment under water vapor condition.

The schematic diagram of the experimental equipment is shown in Fig. 2. It mainly consists of three parts, i.e. water vapor generator, heating unit and gas analyzer. For the water containing atmosphere, water was generated by the peristaltic pump at 0.12 mL/min. The water vapor and the carrier gas with the volume ratio of 1:1 were mixed in a 300°C-tank. Then the water containing atmosphere was introduced into the furnace tube (99.99 mass%  $Al_2O_3$ ) with the flow rate of 200 mL/min.

For the isothermal oxidation experiments, the following steps were adopted: The sample about 1 g placed in the high purity alumina crucible was put into the hot zone of the furnace. The reaction tube was flushed with argon for two hours to eliminate air in the furnace. Then the furnace was heated to the required temperature in argon as quickly as possible. Once the thermal equilibrium was obtained, the water containing atmosphere was injected in the reaction tube. The hydrogen concentration in the outlet gas was measured online continuously by a gas analyzer. The phase and the microstructure of the solid product were investigated using various techniques.

In view of the enrichment of the iron oxide, the following procedure was adopted: The solid product of 1 g was mixed with 20 mL 1 mol/L NaOH solution. Then it was put into the autoclave and heated at 180°C for 6 h. The solution was subsequently precipitated, filtered and washed using deionized water, which was repeated for three times. Finally the solid product was naturally dried in air and collected.

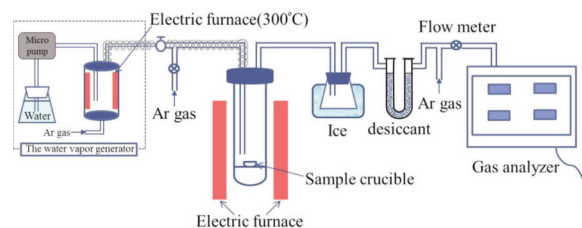


Figure 2. Schematic of the oxidation experimental set-up



### 2.3. Phase and morphology characterization

The phase composition of the specimen and the reaction product were characterized by X-ray diffractometer (XRD; Ultima IV, Rigaku, Japan) using Cu K $\alpha$  radiation ( $\lambda = 1.5406 \text{ \AA}$ ) with a step size of  $0.02^\circ$ . Rietveld refinement was performed using TOPAS 4.2 software (Bruker AXS, Berlin, Germany) to quantitatively calculate the content of solid products. The microstructure of the specimen and the reaction product were observed on a scanning electronic microscope (SEM; SUPRA 55, ZEISS, Germany) equipped with an energy dispersive spectrometer (EDS; INCA250, Oxford Instruments, UK). The hydrogen concentration in the outlet gas was measured online continuously by a gas analyzer (Ibrid MX6, Industrial Scientific, Oakland, PA, USA).

## 3. Results and discussion

### 3.1. Sample characterization

XRD powder diffraction patterns of the synthesized fayalite are shown in Fig. 3. It can be seen that all the characteristic peaks correspond to fayalite phase. No other phase is detected. Fig. 4 shows the SEM images with EDS analysis of the obtained specimen. Fig. 4a shows the microstructure of the sintered specimen at low magnification. It can be seen

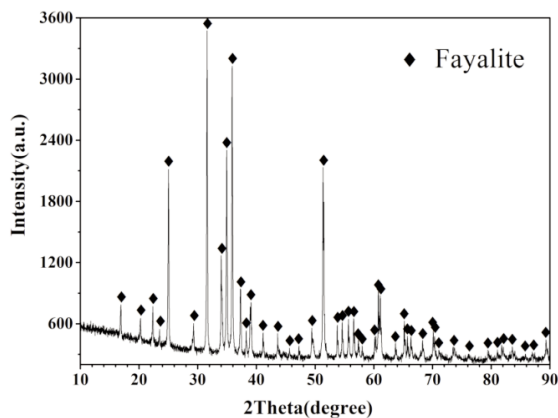


Figure 3. XRD patterns of the synthesized fayalite at  $1150^\circ\text{C}$  for 5 h in air

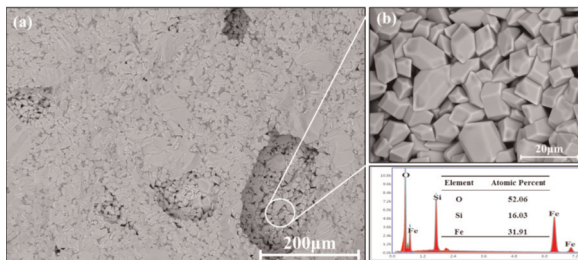


Figure 4. SEM images at low (a) and high magnification (b) and corresponding EDS mapping of elements analyzed of the synthesized fayalite

that the microstructure is uniform and the grains contact tightly together. At high magnification (Fig. 4b), the grains are characterized as wedge-shaped particles. The corresponding EDS mapping analysis indicates that the chemical compositions are Si, Fe and O with the atom ratio of 1: 2: 3.25, which is close to the stoichiometric ratio of  $\text{Fe}_2\text{SiO}_4$ . This is in consistent with the XRD analysis (Fig. 3).

### 3.2. Oxidation behavior of fayalite in water vapor

#### 3.2.1. Characterization of solid products

XRD analysis was carried out to analyze the phase development of the samples before and after reaction. The results shown in Fig. 5 indicate that the phases of magnetite, hematite and silica appear when exposed to water vapor at  $1000^\circ\text{C}$  for 20 min. With the oxidation time extending, the relative intensity of the characteristic peaks of the above three phases are obviously enhanced. The characteristic peaks of fayalite disappear after being oxidized for 40 min, indicating the processes of oxidation and decomposition of fayalite has finished. When the oxidation time is extended to 50 min, the relative intensity of the characteristic peaks of hematite increases. The quantitative analysis of the solid product content is calculated by adopting TOPAS 4.2 software and the results are presented in Fig. 6. It can be seen that the total amount of magnetite is 58.8 wt% after being oxidized for 40 min. Then the amount of magnetite decreases to 42.1 wt% when the oxidation time is extended to 50 min. At the same time, the fraction of hematite and silica crystals increases a little. The possible reason is that magnetite is further oxidized to form hematite with the extension of oxidation time. As for silica, the crystallization phase also increases with increasing the oxidation time. Since magnetite is a valuable product and has lots of industrial applications, the recover the magnetite from the mixed product of magnetite and hematite, it can be separated by magnetic separation according to different industrial applications demands.

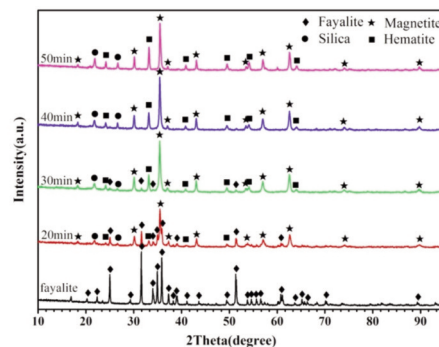
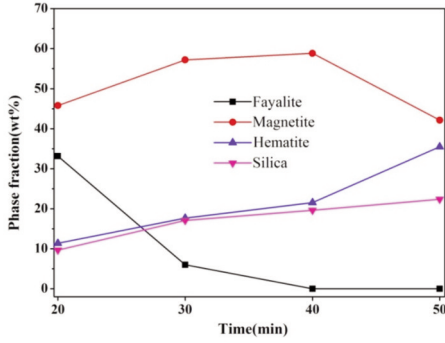
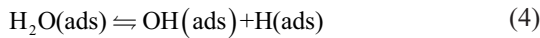


Figure 5. XRD patterns of fayalite powder before and after reaction with water vapor at  $1000^\circ\text{C}$  for different time



**Figure 6.** Quantitative analysis of the solid product content of fayalite powder after reaction with water vapor at 1000 °C for different time

For comparison, XRD pattern of fayalite oxidized at 1000 °C for 40 min in dry air was also analyzed. As shown in Fig. 7, it can be seen that the phases are mainly hematite and silica after oxidation in dry air. This indicates that water promotes the formation of magnetite. The reasons can be attributed to as follows. According to the phase diagram [21] (Fig. 8), the oxygen fugacity is fixed at 0.21 atm when the oxidation experiment is performed in air at 1000 °C (point A in Fig. 8). Hematite is the stable iron oxide phase under this condition. When fayalite exposed to water at high temperature, it provides a catalytic surface for water vapor adsorption. Water molecules first undergo a physisorption process and upon interaction between Fe 3d-orbitals and water O 2p-orbitals, a weak substrate-adsorbate bond is created. Subsequently, water molecules dissociate into OH and H surface species, where the OH groups reside on the metal atoms and the H species are attached to the O atoms surface. And OH dissociates to produce adsorbed oxygen atoms [26-29]. The process can be expressed as follows:



The active H can easily enter fayalite because of its smaller radius and shift the H–O–H<sub>2</sub>O equilibration as follows [30]:



$$K = \frac{N_{\text{H}}^2 N_{\text{O}}}{P_{\text{H}_2\text{O}}} \quad (7)$$

$$N_{\text{O}} = K \frac{P_{\text{H}_2\text{O}}}{N_{\text{H}}^2} \quad (8)$$

Where the underlines represent species in solution in fayalite,  $N_{\text{O}}$  is the oxygen solubility in the sample, and  $K$  is the equilibrium constant. For a given partial pressure of water vapor, the local oxygen

concentration varies as the inverse square of the hydrogen concentration. Initially water vapor dissociates into active  $\text{H}$  and  $\text{O}$ , and a hydrogen molecule forms through the recombination of two adsorbed hydrogen atoms [31]. Hydrogen concentration continuously increases while the dissolved oxygen concentration is reduced according eq 8. Therefore the oxygen fugacity can be controlled under the magnetite-hematite phase boundary (MH) as shown in area B in Fig. 7. As a consequence, magnetite is promoted as the main iron oxide product. With time extending, the oxidation and decomposition of fayalite completes and hydrogen concentration is reduced. Thus the concentration of dissolved oxygen is increased and magnetite mainly reacts with water to form hematite. Therefore more factors should be adopted to control the oxygen fugacity to obtain magnetite besides water vapor. More work will be carried out in the future.

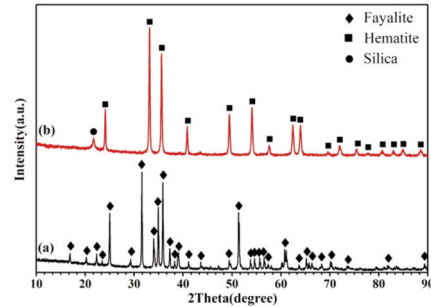


**Figure 7.** XRD patterns of fayalite before (a) and after oxidation (b) at 1000 °C for 40 min in dry air

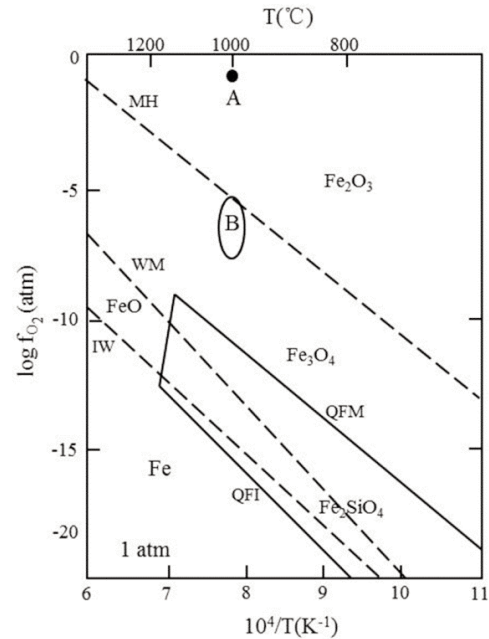


**Figure 8.** Phase diagram in temperature and oxygen fugacity space for fayalite and the iron-oxygen system [21]

The microstructure development of fayalite powder before and after oxidation under water vapor containing condition at 1000 °C for different time is shown in Fig. 9. Compared with fayalite powder before reaction (Fig. 9a), a significant observation is the growth of a specific structure on the surface of fayalite particle after reaction. As shown in Fig. 9b, some smaller bumps are formed on the surface of fayalite particle after oxidation for 20 min. At high magnification (inset in Fig. 9b), the bump is a compact granular layer. Based on EDS mapping analysis, the compact granular layer predominately consists of iron oxide while with tiny amounts of silica. In addition, the granule size of the iron oxide significantly increases as the oxidation time increasing (Fig. 9c-d).

For the detailed morphology of the oxidation product, the SEM images of the solid product after oxidation for 40 min at high magnification are shown in Fig. 10. It can be seen that the oxide grains possess the spinel shape, which is the characteristic of

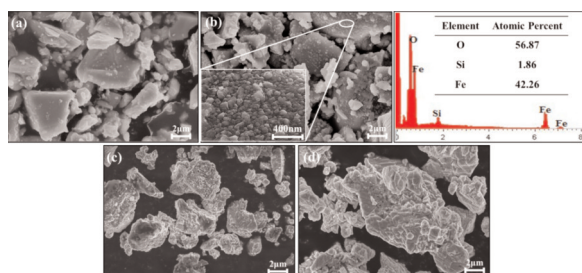


**Figure 9.** SEM images of fayalite powder before and after reaction at 1000 °C for different time (a) 0min, (b) 20 min, (c) 30 min and (d) 40 min

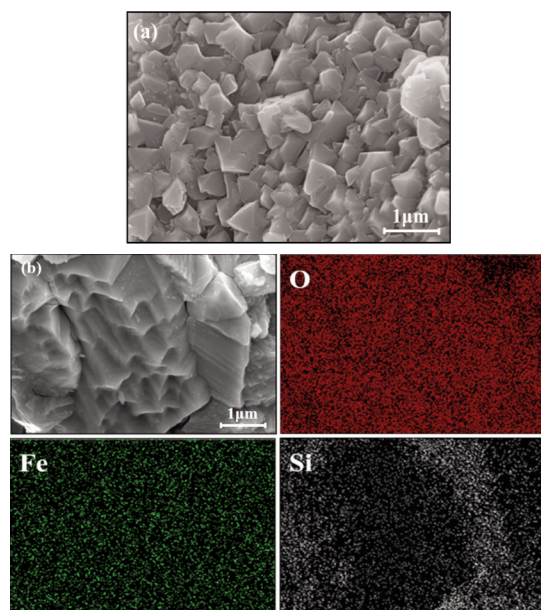


**Figure 10.** SEM images and the corresponding EDS analysis of the oxidation solid product at 1000 °C for 40 min

magnetite (Fig. 10a). From the corresponding EDS mapping of elements analysis (Fig. 10b), silica exists in the form of very tiny particles and mainly distributes on the top of magnetite, further verifying water vapor can promote fayalite to transform into magnetite.

### 3.2.2. Characterization of gas product

The hydrogen generation during the oxidation when exposed to water vapor is investigated. Fig. 11 shows the hydrogen concentration as a function of time during the oxidation process. The time lag between water injection and hydrogen detection is the sampling time and the gas analyzer response time. It is characterized as typically three stages. In the first stage, the hydrogen concentration in the off-gas increases rapidly to a maximum value just in few seconds. Then the production rate levels off for about 1000 s. In the third stage, the hydrogen concentration decreases rapidly. Combining the XRD analysis, the oxidation reaction should complete in this stage. In this work, the fayalite particles produce 24.41 mL of hydrogen per gram at 1000 °C for 40 min in 50 vol% water vapor–50 vol% Ar. Compared with the hydrogen production by water splitting thermochemical cycle based on transition metal oxide redox pair, for instance, Christopher L. Muhich et al [32] reported isothermal water splitting at 1350 °C using the “hercynite cycle” with H<sub>2</sub> production capacities of 2.28 mL/g•cycle. Jonathan R. Scheffe et al [33] investigated spinel ferrite/hercynite water-splitting redox cycle and the H<sub>2</sub> production is 11.2 mL/g•cycle at a reduction temperature of 1200 °C. Rahul R. Bhosale et al [34]. reported water-splitting for H<sub>2</sub> generation using sol-gel derived Mn-ferrite with an average of 8.44 mL g<sup>-1</sup>•cycle-1 H<sub>2</sub> at water splitting temperature of 900 °C. The hydrogen production capacity in our study is superior to the reported results in the literature. The possible reason is that the number of reduced iron (Fe<sup>2+</sup>) dictates the total H<sub>2</sub>-generating capacity

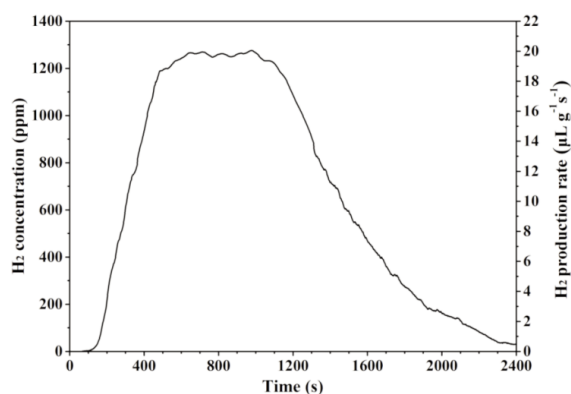


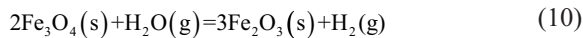
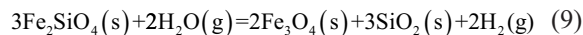
**Figure 11.** The hydrogen concentration as a function of time during the oxidation process at 1000 °C



of fayalite with a maximum ratio of one H<sub>2</sub> molecule produced to every two Fe<sup>2+</sup> cations. In this experiment, fayalite contains abundant Fe<sup>2+</sup>, which provides the essential conditions for hydrogen production. In addition, the reaction is sufficient so that most of the Fe<sup>2+</sup> ions are oxidized to Fe<sup>3+</sup> during the 40 min.

### 3.2.3. Reaction mechanism

From the above experimental results, the oxidation process of fayalite with water vapor at high temperature can be expressed as follows:



With time further prolonging, certain amount of magnetite can be further oxidized into hematite. The reaction mechanism is shown in Fig. 12. At high temperature, water vapor adsorbs on the surface of fayalite and decomposes to form active H and OH. OH dissociates to produce adsorbed oxygen atoms. The overall process can be expressed as eqs 3-5. The active H can easily enter the sample because of its smaller radius and shift the H–O–H<sub>2</sub>O equilibration as expressed by eqs 6-8. Initially hydrogen concentration in fayalite continuously increases because the active H can easily enter the sample. This leads the dissolved oxygen concentration in fayalite to reduce and the oxygen fugacity can be controlled under the magnetite-hematite phase boundary (MH) as shown in area B in Fig. 7. Therefore the content of magnetite domains among the solid products. After certain time, the oxidation and decomposition of fayalite completes and hydrogen concentration is reduced. Thus the concentration of dissolved oxygen is increased and magnetite mainly reacts with water to form hematite.

### 3.3. Enrichment of the iron oxide

To further enrich the iron oxide, the oxide mixture was treated via alkaline cleaning in 1 mol/L NaOH for 6 h. XRD pattern of the products before and after treatment with NaOH solution were analyzed as shown in Fig. 13. The characteristic peaks of SiO<sub>2</sub> disappeared after treatment with NaOH solution, indicating that silica contained in the oxidation products can be removed by the following reaction [35]:



The quantitative analysis of the solid product content is calculated by adopting TOPAS 4.2 software and the results are as follows (wt%): magnetite, 70.7; hematite, 28.89; SiO<sub>2</sub>, 0.33; Na<sub>2</sub>O, 0.05 respectively. SiO<sub>2</sub> and Na<sub>2</sub>O are in relative low content. It shows that the iron oxide can be further enriched via alkaline cleaning in 1 mol/L NaOH.

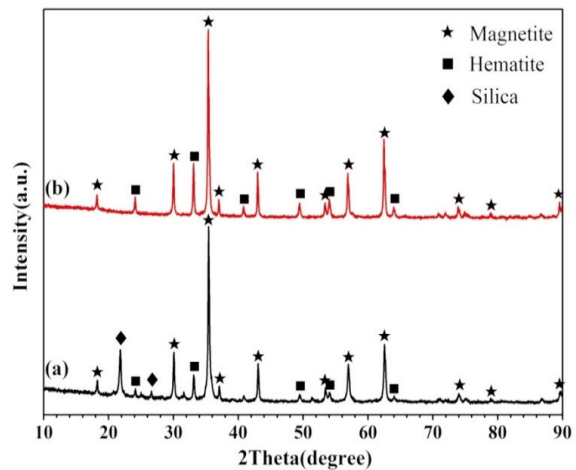


Figure 13. XRD patterns of the solid product before (a) and after treatment (b) with NaOH solution

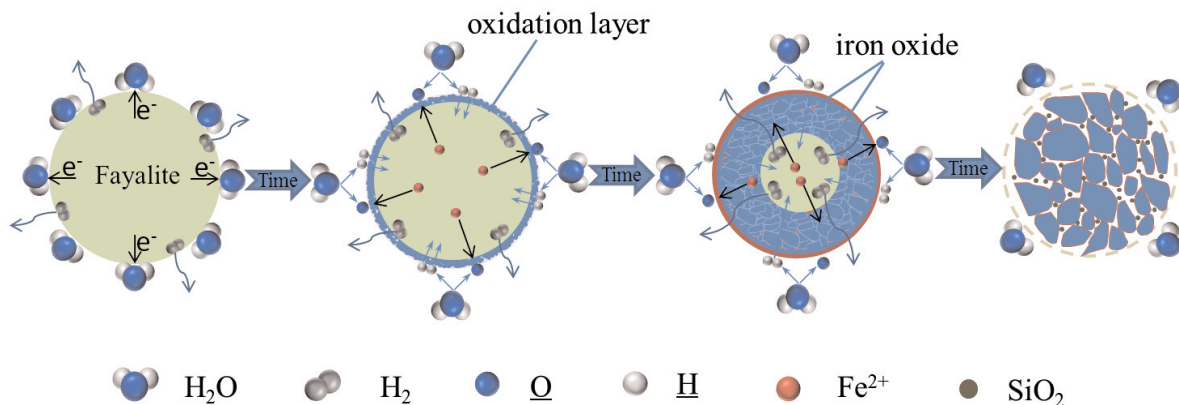
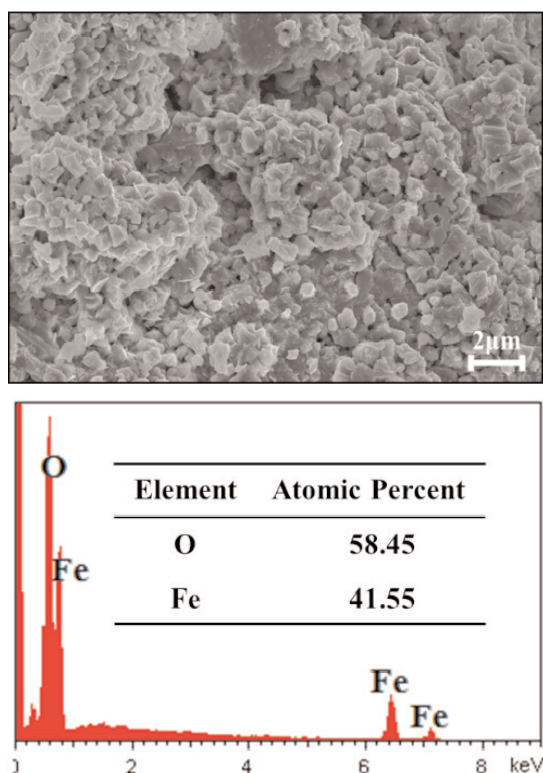


Figure 12. The schematic of the reaction process of fayalite powder exposed to water vapor at high temperature

SEM and the corresponding EDS mapping of elements analysis of the solid product after treatment with NaOH solution are performed as shown in Fig. 14. From the corresponding EDS mapping of elements analysis, the obtained solid product after treatment with NaOH solution is iron oxide. This is in agreement with the XRD analysis (Fig. 13b). In this way, iron oxide and silica were separated completely and those can be used as iron concentrate, catalyzer, abrasive materials and source of water glass production, respectively.



**Figure 14.** SEM images and the corresponding EDS analysis of the solid product after treatment with NaOH solution

#### 4. Conclusions

In this work, fayalite was exposed to water vapor at 1000 °C for different time. The solid products are magnetite (58.8 wt%), hematite (21.6 wt%) and silica (19.6 wt%) at 1000 °C for 40 min. At the same time 24.41 mL/g hydrogen can be produced. The iron oxide product can be further enriched with NaOH solution. As for the reaction mechanism, water vapor can promote fayalite to transform into magnetite by decreasing the oxygen fugacity condition of the system as well as shifting the H–O–H<sub>2</sub>O equilibration. This is beneficial for the further separation and enrichment of iron oxide.

#### Acknowledgement

This study was supported by the National Science Fund for Excellent Young Scholars of China (No.51522402), the National Natural Science Foundation of China (No.51572019 and U1460201), the Special Fund of the National Excellent Doctoral Dissertation (No.201437) and the Central Universities of No. FRF-TP-15-006C1.

#### References

- [1] H. Shen and E. Forsberg, Waste Manage., 23 (10) (2003) 933-949.
- [2] M.G. Bodas and S.B. Mathur, Ind. Eng. Chem. Res., 36 (12) (1997) 5419-5424.
- [3] A.N. Banza, E. Gock and K. Kongolo, Hydrometallurgy, 67 (1-3) (2002) 63-69.
- [4] K. Murari, R. Siddique and K.K. Jain, J. Mater. Cycles waste Manag., 17 (1) (2015) 13-26.
- [5] X.L. Zhou, D.Q. Zhu, J. Pan and T.J. Wu, ISIJ Int., 55 (7) (2015) 1347-1352.
- [6] A. Wolf and A.M. Mitrašinović, J. Min. Metall. B., 52 (2) (2016) 143-150.
- [7] Z.Y. Lan, X.J. Li, S.Q. Liu, W.P. Wang and M. Zhang, Adv. Mater. Res., 753-755(2013) 44-47.
- [8] B. Gorai, R.K. Jana and Premchand, Resour. Conserv. Recy., 39 (4) (2003) 299-313.
- [9] D.S. Rao, S. Angadi, and P.S.R. Reddy, J. Inst. Eng. India Ser. D., 96 (1) (2015) 7-13.
- [10] G. Stoyko, K. Yoanna, K. Galina and I. Anna, Waste Manage. Res., 29 (2) (2011) 157-164.
- [11] M. Cococcioni, A.D. Corso and S.D. Gironcoli, Phys. Rev. B., 67 (9) (2003) 552-555.
- [12] K. Ullrich, K. Langer and K.D. Becker, Phys. Chem. Minerals., 29 (29) (2002) 409-419.
- [13] C. Davoisne and H. Leroux, Nucl. Instrum. Methods. Phys. Res. B., 243 (2) (2006) 371-376.
- [14] S.J. Bai, S.M. Wen, D.W. Liu and W.B. Zhang, Can. Metall. Quart., 51 (4) (2012) 376-382.
- [15] Y. Fan, E. Shibata, A. Iizuka, and T. Nakamura, J. MMIJ., 129 (5) (2013) 177-184.
- [16] B.S. Kim, S.K. Jo, D. Shin, J.C. Lee and S.B. Jeong, Int. J. Miner. Process., 124 (3) (2013) 124-127.
- [17] J. Palacios and M. Sánchez, Miner. Process. Extr. Metall., 120 (4) (2011) 218-223.
- [18] Y. Fan, E. Shibata, A. Iizuka and T. Nakamura, Metall. Mater. Trans. B., 46 (5) (2015) 2158-2164.
- [19] K.Q. Li, S. Ping, H.Y. Wang, W. Ni, Int. J. Min. Met. Mater., 20 (11) (2013) 1035-1041.
- [20] D. Busolic, F. Parada, R. Parra, M. Sanchez, J. Palacios and M. Hino, Miner. Process. Extr. Metall., 120 (1) (2011) 32-36.
- [21] S.J. Mackwell, Phys. Chem. Minerals., 19 (4) (1992) 220-228.
- [22] U. Brinkmann and W. Laqua, Phys. Chem. Minerals., 12 (5) (1985) 283-290.
- [23] I. Gaballah, S.E. Raghy and C. Gleitzer, J. Mater. Sci., 13 (9) (1978) 1971-1976.
- [24] S. Gyurov, D. Rabadjieva, D. Kovacheva and Y.



- Kostova, J. Therm. Anal. Calorim., 116 (2) (2014) 945-953.
- [25] E.H. Wang, H. Dong, J.H. Chen, K.C. Chou and X.M. Hou, Oxid. Met., 84 (1-2) (2015) 169-184.
- [26] S.R.J. Saunders, M. Monteiro and F. Rizzo, Prog. Mater. Sci., 53 (5) (2008) 775-837.
- [27] C.T. Fujii and R.A. Meussner, J. Electrochem. Soc., 111 (11) (1964) 1215-1221.
- [28] A.P. Grosvenor, B.A. Kobe and N.S. McIntyre, Surf. Sci., 572 (2-3) (2004) 217-227.
- [29] C.G. Zhou, Q.F. Zhang, L. Chen, B. Han, G. Ni, J.P. Wu, D. Garg and H.S. Cheng, J. Phys. Chem. C., 114 (49) (2010) 21405-21410.
- [30] Y. Joseph, C. Kuhrs, W. Ranke, M. Ritter and W. Weiss, Chem. Phys. Lett., 314(3-4) (1999) 195-202.
- [31] F. Kosaka, H. Hatano, Y. Oshima and J. Otomo, Chem. Eng. Sci., 123(2015) 380-387.
- [32] C.L. Muhich, B.W. Evanko, K.C. Weston, P. Lichty, X.H. Liang, J. Martinek, C.B. Musgrave and A.W. Weimer, Science., 341 (6145) (2013) 540-542.
- [33] J.R. Scheffe, J.H. Li and A.W. Weimer, Int. J. Hydrogen Energ., 35 (8) (2010) 3333-3340.
- [34] R.R. Bhosale, R.V. Shende and J.A. Puszynski, Int. J. Hydrogen Energ., 37 (3) (2012) 2924-2934.
- [35] G.A. Gyurov, C.G. Georgiev, M.H. Belomorski and S.A. Gyurov, European Patent 2331717B1 (2012).

## ISKORIŠĆENJE OKSIDA GVOŽĐA IZ FAJALITA POMOĆU VODENE PARE NA VISOKIM TEMPERATURAMA

J.H. Chen <sup>a</sup>, W.J. Mi <sup>a</sup>, H.Y. Chen <sup>a</sup>, B. Li <sup>a</sup>, K.C. Chou <sup>b</sup>, X.M. Hou <sup>b,\*</sup>

<sup>a</sup> Škola nauke o materijalima i inženjerstvo, Univerzitet za nauku i tehnologiju, Peking, Kina

<sup>b</sup> Državna laboratorija napredne metalurgije, Univerzitet za nauku i tehnologiju, Peking, Kina

### Apstrakt

Oksidaciono ponašanje fajalita ( $Fe_2SiO_4$ ) u vodenoj pari na temperaturi od 1000°C, ispitivano je u radu. Sastav faza i mikrostruktura čvrstih produkata su ispitani rendgenskom difrakcijom (XRD) i skenirajućim elektronskim mikroskopom (SEM) koristeći energetska disperzivni spektrometar (EDS). Gasoviti produkt je kontinuirano meren gasnim analizatorom. Rezultati su pokazali da se fajalit u potpunosti razlaže na magnetit (58.8 wt%), hematit (21.6 wt%) i silicijum (19.6 wt%) na 1000°C tokom 40 minuta u vodenoj pari. Kada se uporede rezultati dobijeni na suvom vazduhu, dolazi se do zaključka da vodena para može da podstakne transformaciju fajalita u magnetit smanjenjem fugaciteta kiseonika. Pored toga, produkt oksida gvožđa je obogaćen baznim prečišćavanjem u rastvoru 1 mol/L NaOH. Kada je u pitanju produkt gasa, nastalo je 24.41 mL/g vodonika u rastvoru koji je sadržao 50% vode i 50% Ar na temperaturi od 1000°C tokom 40 minuta.

Keywords: Fajalit; Vodena para; Oksidaciono ponašanje; Vodonik; Magnetit.

